Silicon dioxide defects induced by metal impurities

H. Dallaporta,* M. Liehr, and J. E. Lewis
IBM Research Division, Thomas J. Watson Research Center, P.O. Box 218, Yorktown Heights, New York 10598
(Received 18 September 1989)

The decomposition of SiO_2 films on Si(100) during ultrahigh-vacuum anneal is studied in a scanning Auger microscope. Decomposition is found to be strongly enhanced by monolayer amounts of impurities deposited on the SiO_2 surface. *s*- and *p*-band elements initiate decomposition via formation of volatile suboxides by surface reaction. In contrast, most transition metals decompose the oxide via laterally inhomogeneous growth of voids in the oxide, suggesting strongly that they need to diffuse to the SiO_2/Si interface and there enhance oxide decomposition via formation of volatile SiO. It is hypothesized that existing defects in the oxide layer, enhanced by, e.g., film stress, permit metal migration to the interface. The oxide decomposition enhancement found for the transition metals is thought to be related to the electronic properties of those metals, namely, the density of states close to the Fermi level. A strong decrease in reactivity is found upon silicidation of the metal, supporting the above picture.

INTRODUCTION

With higher levels of device integration and complexity an ever increasing number of processing steps is needed in very-large-scale integration materials processing. Imperfect processing conditions tend to introduce defects into a device structure that are exceedingly difficult to characterize because of their low density and small size. Most sensitive to processing-induced electrically active defects are thin insulator layers next to active regions, in particular gate-oxide layers. Our intention in this study is to contribute to the understanding of the physical and chemical processes by which contaminants or particles degrade gate-oxide layers. The deleterious effect of metal contamination on gate oxides has been known for decades and metals have been successfully eliminated from the oxide-growth process by using chlorine additions to the oxygen ambient.[1] Relatively little is known, though, about the chemical reaction between metal contaminants and gate-oxide structures, e.g., which metals are the most reactive and thus most critical to avoid in device processing.

The discovery of a defect-decoration technique[2-6] allows one to correlate physical defects in a gate oxide, namely, the formation of voids during a high-temperature vacuum anneal, with electrical defects in metal-oxide-semiconductor structures. We are going to use this method to elucidate the microchemistry at a SiO_2/Si interface when controlled metal contamination is introduced. From the comparison of the measured reactivity of the different metals, we can derive a model to understand the behavior of these materials toward the SiO_2/Si structure and their role in the modification of the electrical characteristics.

A set of metals has been chosen to cover different thermodynamical and electronic properties (diffusion coefficients, reactivity with SiO_2, electron density of states near the Fermi level). We studied Al and Mg as *s*-type-electron metals, W and Ti as transition metals with few *d* electrons, Pd, Ni, and Pt as nearly fully *d*-shell metals, and finally Cu, Ag, and Au as completed-*d*-shell metals with a large (several eV) separation of the *d* bands and the Fermi level. We have observed one main difference in the decomposition process and we will use this to group the metals in two classes for the discussion. (i) *s*-type, *p*-type, and transition metals with few *d* electrons on one side, and (ii) all other transition metals on the other. *s*-type metals exhibit oxide decomposition that appears laterally uniform on the scale of our experimental resolution ($\simeq 500$ nm), whereas all other metals lead to formation of voids in the oxide layer as dominant mechanism of oxide decomposition. Formation of voids has been also observed during oxide decomposition by annealing noncontaminated gate-quality SiO_2/Si structures.[2] Voids are formed in the oxide layer upon anneal in oxygen-free ambients (e.g., vacuum), exposing clean silicon and leaving the oxide between the voids intact. Oxide decomposition proceeds by lateral growth of the void via an interfacial reaction between the exposed Si and the oxide at the void perimeter through the chemical reaction $Si + SiO_2 \rightarrow 2SiO\uparrow$.[2,7-9]

EXPERIMENTAL CONDITIONS

Experiments were performed in a scanning Auger microscope (SAM) which operates under ultrahigh-vacuum (UHV) conditions and allows observation of the sample in the scanning electron microscopy (SEM) mode during annealing at high temperature.[10] Thin films were deposited on 200-Å thermal gate oxide by *in situ* evaporation of the chosen metal from a hot tungsten wire, while thick W films were prepared *ex situ*. For comparison with "clean" conditions, metal films were evaporated only on half of the sample using a shadow mask. Film thickness

was measured with a quartz crystal microbalance. Samples were annealed to 1000 °C in UHV by direct current flow and the temperature was monitored with an infrared pyrometer. The annealing was interrupted during Auger-electron spectroscopy (AES) and SAM data aquisition.

For the class of void-forming metals, void density has been measured in SEM photographs, and from this the void diameter was measured as a function of time. In all cases the void diameter was found to grow linearly with time.[10] To obtain a time-independent measure of the decomposition rates the void diameter growth rate has, therefore, to be taken, instead of the void area growth rate. To quantify relative rates of oxide decomposition for different metals, which involve different void densities and growth rates, we define a linear decomposition rate (LDR) as the product of the density of voids and the void diameter growth rate. We shall deduce the reactivity for each metal by dividing this product by the film thickness.

To test the effects of metal diffusion either through the bulk oxide or the silicon, three different experiments were performed. (1) Deposition of the metal film on top of the oxide; (2) prediffusion of the metal through the oxide by annealing at 500 °C in 1 atm of nitrogen (this treatment enhances metal diffusion in bulk oxide[11]); (3) use of a silicon wafer with a polysilicon getter on the backside, which diminishes the metal atom density at the SiO_2/Si interface by trapping metal atoms in the backside getter instead of at the interface.[12,13] All three pretreatments were followed by a standard anneal to 1000 °C in a vacuum of better than 10^{-8} Torr.

Furthermore, samples with 1500 Å WSi_2 on Si(100) were used as substrates for thermal oxidation. 200 Å thermal oxide was grown on them in 1 atm oxygen at 800 °C. WSi_2 was chosen because of its thermal stability under anneal to 1000 °C and its ability to grow a stoichiometric SiO_2 upon thermal oxidation.[14] On another set of samples, 500 Å thick tungsten dots were deposited *ex situ* through a shadow mask on high-quality thermal oxide. Both kinds of samples were loaded into the SAM and subjected to the high-temperature vacuum anneal without any further pretreatment.

RESULTS

Magnesium, aluminum, titanium, silicon, and germanium

We first deal with one class of materials (Al, Mg, Ti, Si, and Ge), which is distinguished from the other class by its reactivity towards SiO_2. To illustrate the properties of this class of materials we choose Al as an example; all others behave very similar. A 35-Å-thick Al film annealed for 120 sec to 1000 °C decomposes a 200 Å thermal oxide as shown in the SEM picture in Fig. 1(b). The picture shows a uniform surface with no recognizable structure within the resolution of the instrument ($\simeq$500 nm). Anneals to intermediate temperatures (e.g., 400 °C) show the formation of silicate at the sample surface. This leads us to believe that the reaction at the surface is even uniform on an atomic scale, not just within the rather limited resolution of our microscope ($\simeq$500 nm).

Even in the case of very low metal coverage, we do not observe inhomogeneity in the oxide layer decomposition. The chemical composition of the surface, as checked with AES, corresponds to a clean silicon surface (no trace of

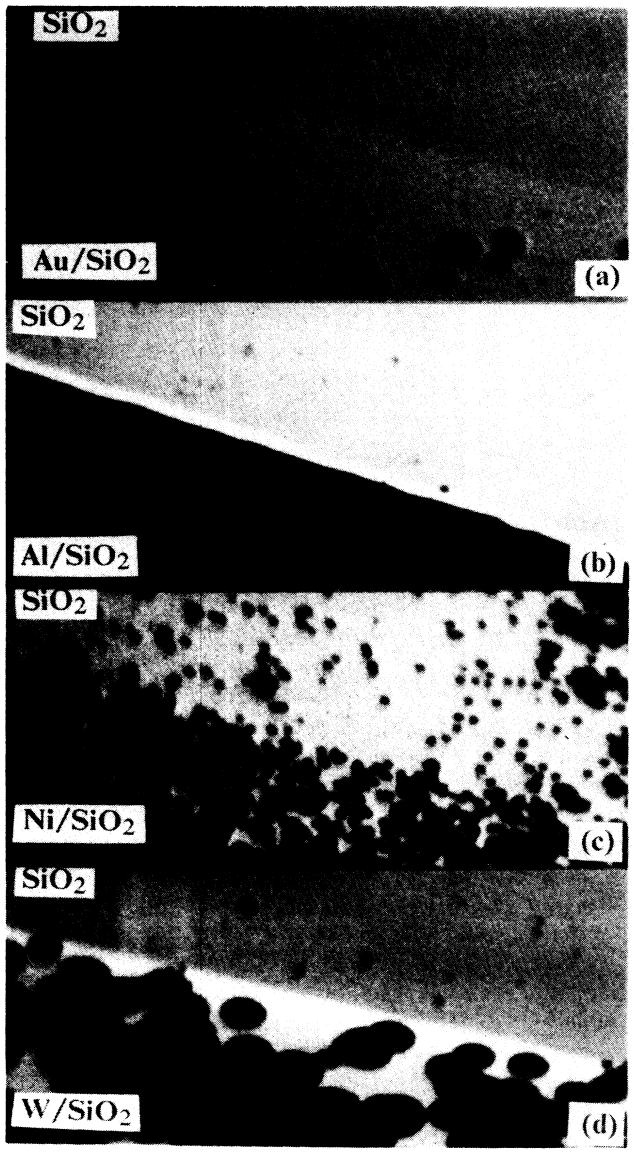

FIG. 1. A sequence of scanning electron microscope pictures taken during ultrahigh-vacuum anneal of a 200 Å SiO_2 layer on Si(100). The field of view is $\simeq$1 mm by 1 mm, the sample being tilted by $\simeq$60° giving circular voids an elliptical appearance. The pictures were taken at 3 keV electron energy and 50 nA beam current in secondary electron mode. The dark areas represent clean Si areas, the bright background the SiO_2 layer. Metals have been evaporated only on the lower half of the samples to allow comparison with clean conditions. (a) shows a layer of 40 Å of Au after anneal to 1000 °C for 15 min; (b) 35 Å of Al after anneal to 1000 °C for 2 min; (c) 3 Å of Ni after anneal to 1000 °C for 50 min; (d) 3 Å of W after anneal to 1000 °C for 30 min.

metal left after annealing). Apparently, the kinetics of the oxide decomposition reaction changes significantly from the case of a clean oxide when Al is deposited on the SiO_2/Si structure. We know from previous studies[10] that it takes $\simeq$20 h to decompose an uncontaminated oxide compared to 120 s for the Al covered oxide. The deposition of Al on the SiO_2 drastically increases the reaction rate. The same increase in decomposition speed without recognizable structure in the surface is found for the other members of this class (Mg, Ti, Si, and Ge) when deposited onto 200 Å SiO_2/Si. The decomposition speed for the different elements is not the same, Ge being the fastest, Si the slowest. For some samples that were covered only with a very thin metal overlayer ($\simeq$20 Å or less), the layered structure was depth profiled after anneal. The Auger depth profile revealed that underneath a thin layer of silicon an oxide layer is left intact. Apparently the metal reacted and evaporated, leaving the more slowly reacting silicon behind at the surface; overall, the oxide layer has been thinned in the process. This interfacial reaction metal with oxide has been observed previously for Ti and Al.[15,16]

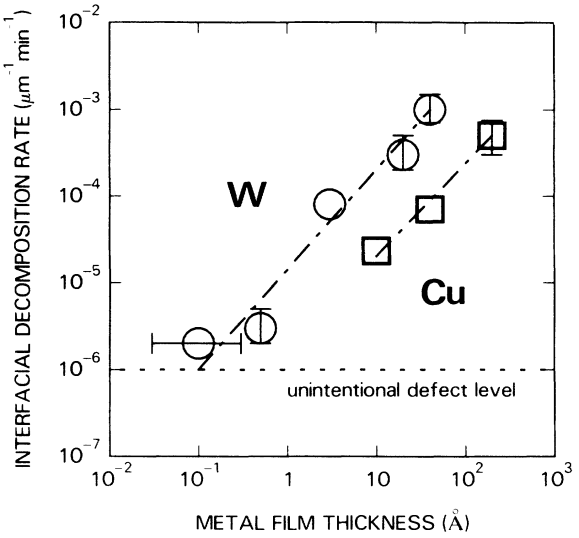

FIG. 2. Oxide decomposition rates measured as linear growth rate of the oxide void diameter times void density vs metal layer thickness. Two examples are chosen, Cu and W. A least-squares fit straight line connects the data points.

Tungsten

Because of the wealth of information available for tungsten, compared to that (only basic decomposition behavior) for the other transition metals, we mention tungsten separately. Figure 1(d) shows the SEM picture of a 3-Å-thick tungsten film deposited on one-half of a 200 Å gate oxide after 30 min annealing to 1000 °C in UHV.[6] On the area previously covered with tungsten an increased density of voids with large diameter is seen, compared to the clean SiO_2 area where only very few, small voids are visible. The elliptic shape of the voids is due to a 60° tilt of the sample with respect to the analyzer. The dark area has been analyzed by AES, and a tungsten silicide is clearly seen when the initial metal layer thickness is above $\simeq$40 Å. The oxide areas between the voids still show unreacted tungsten, but the AES spectra indicate that the film might have aggregated (the ratio of tungsten Auger lines versus silicon Auger lines has changed). The line between the clean oxide surface and the one covered with W is well defined and remains clearly visible even after longer annealing. This seems to indicate that W does not diffuse over significant distances across the surface.

Different tungsten layer thicknesses on identical oxide thicknesses have been annealed under otherwise identical conditions. The LDR at 1000 °C was determined for the different tungsten layers as a function of the thickness, and the results are shown in Fig. 2. The rate of decomposition is found to be a linear function of the amount of metal. The value deduced from a 30 Å thick metal film is $3.7\times10^{-4}/\mu$m min, which is 2 orders of magnitude higher than the value measured for an uncontaminated oxide.

Some of our samples were analyzed with high-resolution transmission electron microscopy (HRTEM). The cross section of a 40-Å-thick tungsten film annealed at 1000 °C for 10 min is shown in Fig. 3. The photograph shows that tungsten aggregated on the SiO_2 surface during the anneal. It is also seen that the oxide thickness remains constant where the decomposition has not started: tungsten does not break through the oxide at every tungsten island. For one W crystal it even looks as if the oxide decomposition front is undercutting the small metal island.

The shape of the void-oxide interface, as seen from above, is shown in detail in the SEM picture in Fig. 4. The picture shows a 30-Å-thick W film at high magnification after 20 min annealing to 1000 °C. A "cauliflower" shape of the void boundary can be seen. This cauliflower void shape has been observed only in the case of tungsten.

For W films over 100 Å, the evolution of the decomposition reaction is quite different and a SEM picture taken from such a sample is shown in Fig. 5. For this particular sample the tungsten film had been patterned by evaporating it through a shadow mask. The dot of tungsten shown in the picture appears structured after anneal; AES shows that tungsten in the middle is surrounded by tungsten silicide. The dark zone at the edge corresponds to clean silicon. Significant decomposition of exposed oxide is observed mainly very close to the dot pattern. A similar reaction has been reported for Au/SiO_2.[17]

As will be discussed later, the enhancement of oxide decomposition found for tungsten requires the metal to reach the Si/SiO_2 interface. To address the question, what large quantities of metal at the interface would do to the decomposition process, we used thermally oxidized tungsten silicide films as substrates. At the temperatures involved tungsten forms silicide when in contact with silicon, and pure tungsten films beneath an oxide cannot be prepared. The silicide is, of course, chemically different from the metal tungsten that we deposited *in situ* on top

FIG. 3. High-resolution cross-sectional TEM photograph of a 40-Å-thick tungsten layer evaporated on 200 Å of thermal oxide. The sample was vacuum annealed to 1000 °C for 10 min.

of the oxide. The silicide had been thermally oxidized at a temperature of 800 °C to give 200 Å of thermal SiO_2 on top of the silicide. A 1500 Å WSi_2 with a 200 Å oxide on top has been annealed to 1000 °C and the SEM picture resulting from the anneal is shown in Fig. 6. The surface exhibits voids, like samples that had pure tungsten evaporated on top of clean oxide. The decomposition rate is not very different from the value obtained for very thin tungsten films deposited on SiO_2.

Noble and quasinoble metals

We now consider the cases of Ni, Pd, Pt, Cu, Ag, and Au. In Fig. 1 we have grouped different SEM pictures

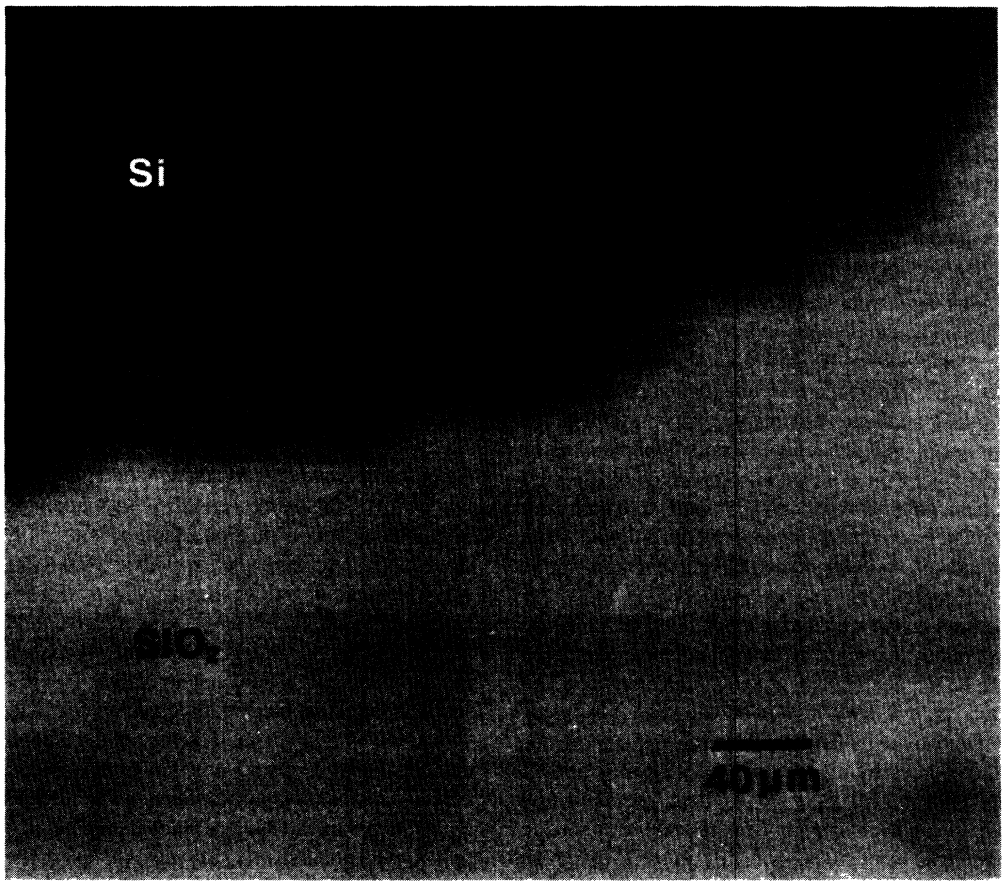

FIG. 4. High-resolution SEM picture of a void edge on a sample with 30 Å tungsten on 200 Å thermal oxide. The sample had been vacuum annealed for 20 min to 1000 °C.

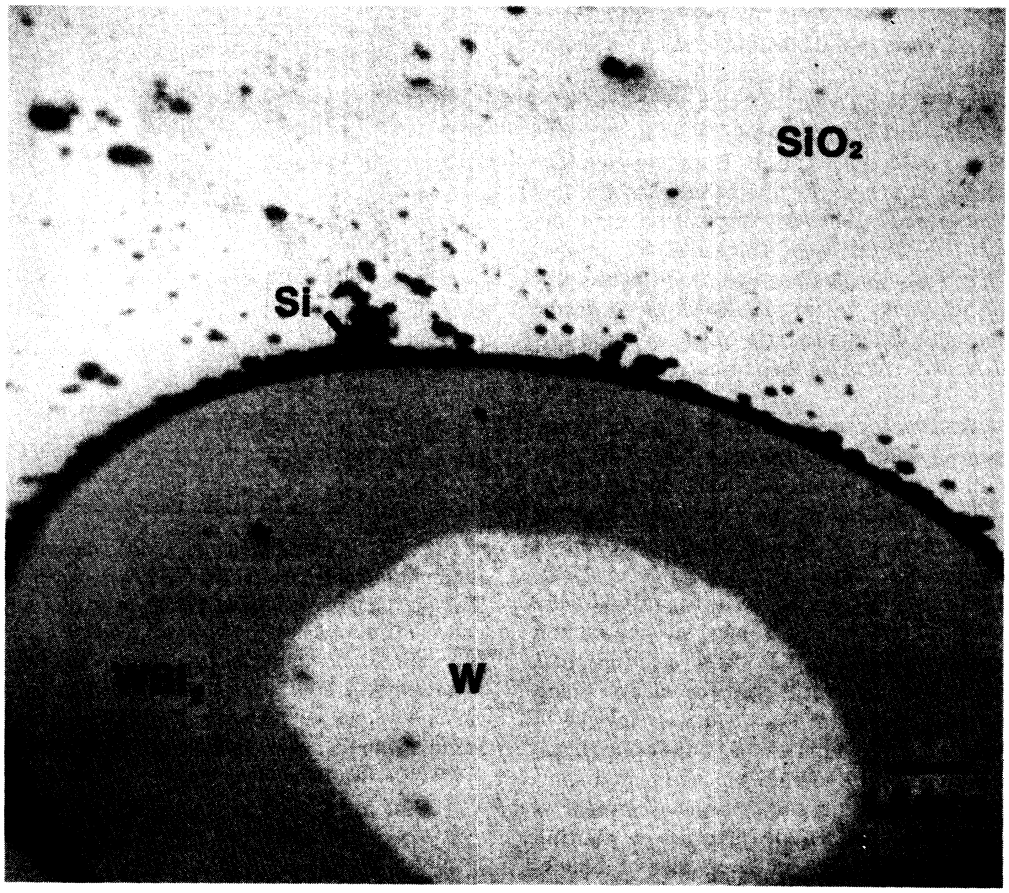

FIG. 5. SEM picture of a 500-Å-thick tungsten dot on 200 Å thermal oxide. The sample has been vacuum annealed to 1000 °C for 12 min. Results of Auger-electron spectroscopic analysis of different areas are indicated.

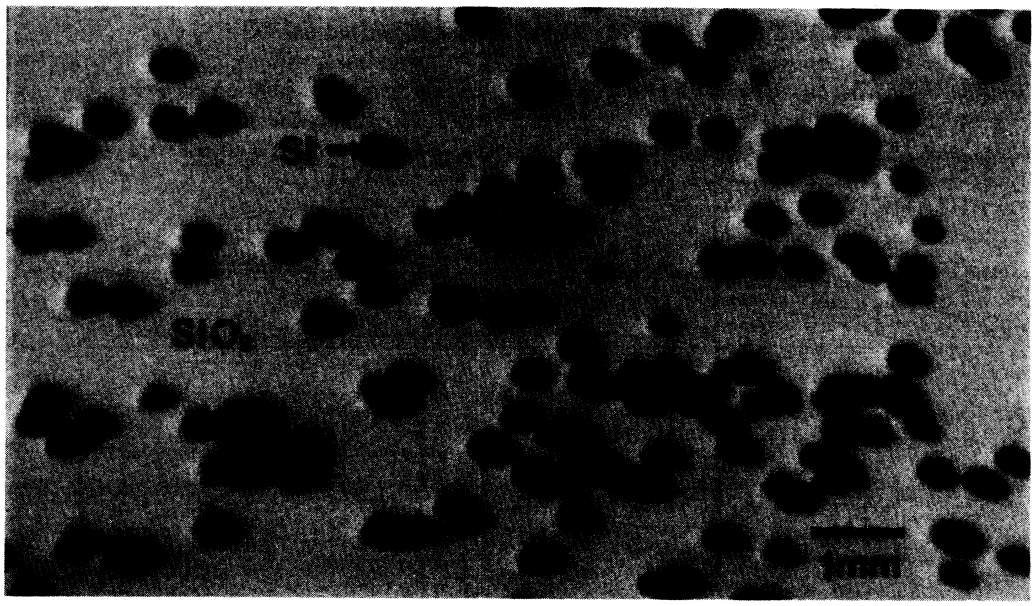

FIG. 6. SEM picture of a Si(100) sample with 1500 Å WSi_2 and 200 Å thermal oxide on top of the silicide. The sample has been vacuum annealed to 1000 °C for 360 min.

for some of those metals together, to reveal differences more clearly. All of these metals decompose an oxide via void formation, so we want to compare different behavior by calculating their LDR. To get a valid comparison of the reactivity, it was verified that the LDR is linear with the film thickness. The case of copper is shown together with tungsten in Fig. 2; a straight line parallel to the line for tungsten is obtained. The decomposition rate depends linearly on the metal layer thickness for copper and tungsten. This behavior has been verified for the other metals also. This linear variation allows us to derive the reactivity of a metal independently of the original layer thickness, provided the film becomes discontinuous during anneal.

The metal reactivities are compared in Fig. 7. Three different experimental conditions are realized in this plot. (1) Thin metal films ($\simeq$3 Å–30 Å) were annealed in UHV to 1000 °C (open circles in the plot). (2) Identical films were annealed first in 1 atm of clean nitrogen to 500 °C, and subsequently annealed to 1000 °C in UHV (black dots in the plot). For Ni and Cu, thin films were deposited on silicon wafers with a polycrystalline silicon backside getter (open squares). The dotted line indicates the oxide decomposition rate measured for clean silicon oxide. The data trend goes from low reactivity for Ag to high reactivity found for Pt. This trend is maintained, although less strikingly, for the nitrogen preannealed samples. The change in the reactivity upon preanneal is more pronounced for metals which have a low melting point and a high vapor pressure. The presence of a backside getter is seen to decrease reactivity for the two cases studied in this way: Cu and Ni.

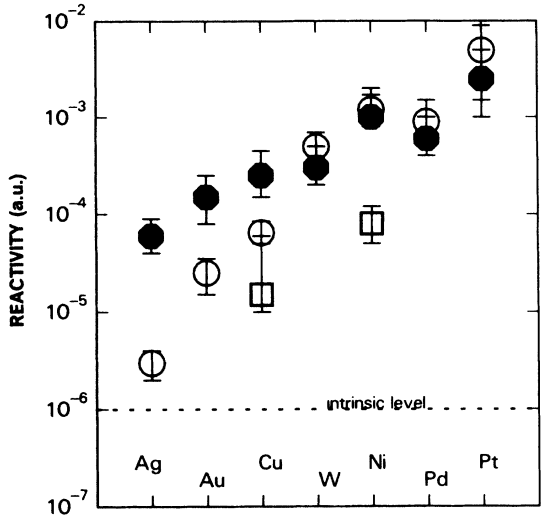

FIG. 7. Comparison of oxide decomposition rates for different metals that decompose 200 Å oxide via void formation. The product of void diameter growth rate and void density—called reactivity in the figure—is chosen as a parameter. The rates are for a metal layer thickness of 1 monolayer. Metals are arranged to exhibit a trend in decomposition rate. Experimental conditions were chosen as all vacuum anneal to 1000 °C (open symbols) or including an inert ambient preanneal to 500 °C for 30 min (solid symbols).

DISCUSSION

Based on the experimental results, the metals we studied can be classified according to two distinctly different reaction pattern upon high-temperature vacuum anneal. For Mg, Al, Ti, and well as Si and Ge, our results show clearly that within the resolution of the SEM ($\simeq$500 nm) the oxide decomposition proceeds with high efficiency by a homogeneous mechanism [Fig. 1(b)]. In the second class of materials (Ag, Au, Cu, W, Ni, Pd, and Pt) the decomposition process is highly inhomogeneous and proceeds via void generation and lateral void growth [Figs. 1(a)–1(c)]. Formation of voids has been also observed during oxide decomposition by annealing gate-quality SiO_2/Si structures which were not intentionally contaminated by metals.[2] The void density and the void growth rate for the deliberately contaminated samples depend strongly on the kind of metal and on the film thickness deposited on SiO_2.

The striking difference between the two classes of materials can be explained in a straightforward manner by comparing the thermodynamic properties of those materials as shown in Table I.[11,18] The first class of materi-

TABLE I. Some selected thermodynamic properties of metals studied here.

Metals	Oxidation	Melting point (°C)	Diffusivity[a] (cm/sec)	Reaction with SiO2	Electronegativity	Heat of reaction[b]	Electronic heat capacity (mJ/mol K)
Al	Yes	660		Yes	1.5	−	
Mg	Yes	650		Yes	1.5	−	
Ti	Yes	1668		Yes	1.2	−	
W	Yes	3410	2×10^{-6}	No	1.7	+	1.3
Ni	Yes	1453	2×10^{-4}	No	1.8	+	7.02
Pd	Yes	1552	5×10^{-5}	No	2.2	+	9.42
Pt	No	1769	3×10^{-6}	No	2.2	+	6.8
Cu	Yes	1083	1×10^{-4}	No	1.9	+	0.695
Ag	Yes	960	2×10^{-8}	No	1.9	+	0.646
Au	No	1063	8×10^{-5}	No	2.4	+	0.729

[a]Diffusivity calculated for neutral species at 900 K in bulk SiO_2 (Ref. 11).
[b]Heat of reaction calculated for reactions involving metal oxide and silicide formation (Ref. 18).

als interact strongly with SiO_2 because they have thermodynamically favorable reaction products.[19,20] At moderate temperatures ($\simeq$400 °C) those materials react with SiO_2 to yield an oxidized metal species, a silicide, and/or a silicate at the surface or the metal-SiO_2 interface. The metals of the second class of materials do not have any thermodynamically favorable reaction products with SiO_2. The coalescence of the tungsten film (Fig. 3) gives a good example for the consequences of a lack of reactivity with the smooth substrate. The surface energy is lowered at elevated temperatures by formation of islands; the metal film does not "wet" the surface.[19]

The heat of formation of a reaction product of the metal-SiO_2 reaction can be calculated in some cases.[18] For metal oxide and some silicides the heat of formation is only negative when the electronegativity is less than 1.5, thus reaction with SiO_2 occurs only then (Table I). This classification distinguishes Al, Mg, Ti, Si, and Ge from the other transition metals studied here. For most *s*-band and *p*-band elements, as well as the *d*-band elements in the first columns of the Periodic Table, reactions with SiO_2 have indeed been observed experimentally.[19,21] We observed that those elements with electronegativity less than 1.5 lead to a strong decomposition of the silicon-dioxide layer. The high decomposition rate can be explained by the oxidation of the metal, providing silicon suboxides, silicides, or elemental silicon. Even though the suboxide of the material is in some cases not volatile, it nevertheless enhances oxide decomposition by producing SiO at the surface, which is volatile itself. This mechanism is supported by our finding of a thin reacted layer at the surface on top of remaining oxide for very thin metal coatings.

If a chemical reaction can occur between any atom of metal and the SiO_2 substrate, obviously no nucleation centers are needed. We expect the oxide decomposition reaction then to occur in a laterally uniform way down to atomic scales. Within the quite limited resolution of our microscope this is indeed what we find. Reactions similar to the ones discussed here [with Ga (Ref. 22) and Ge (Ref. 23)] have been used to remove surface oxide from Si(100) surfaces at moderate temperatures prior to molecular-beam-epitaxy silicon deposition.

For the second class of materials the decomposition proceeds quite differently because of the apparent lack of reactivity with the oxide. These metals are expected to enhance oxide decomposition only when they reach the SiO_2/Si(100) interface.[6] Nucleation of the voids at the oxide-Si interface has already been postulated to explain the void formation characteristics for noncontaminated oxide layers.[2,10] Some of our observation strongly support such a mechanism. The decomposition reactivity is a rather drastic function of whether or not the metal atoms can reach the SiO_2/Si interface and stay there. Experiments designed to increase the amount of metal that reach the interface, such as the nitrogen preanneal experiments[11] (Fig. 7, black dots versus open circles), clearly show an enhancement of the reactivity. Significant changes in reactivity are only seen for those metals that have a large probability to evaporate into the gas phase in the initial period of the high-temperature anneal (high vapor pressure). Experiments designed to decrease the amount of metal at the SiO_2/Si interface, such as having a polycrystalline silicon getter at the wafer backside that competes very efficiently with the interface[12,13] for metal atoms, show unambiguously a decrease of the reactivity. The two examples demonstrated here are Ni and Cu, seen as open squares in Fig. 7. The effect of a polysilicon getter, namely, to reduce metal-induced void nucleation, has already been demonstrated for gate-quality oxides, that had not been intentionally contaminated by metals.[5] The polysilicon serves in those cases as a very efficient getter that competes with the interface for metal atoms, and, therefore, keeps the number of void nucleation centers down. We were able to clearly demonstrate here that transition metals need to reach the silicon-SiO_2 interface to cause oxide decomposition.

There are significant reactivity differences among the materials compared in Fig. 7. A comparison has to be based on the experimental points for nitrogen preanneal to exclude as much as possible the rather obvious differences of vapor pressures. To enhance oxide decomposition the metal atoms or ions have to reach the SiO_2/Si interface, stay there for a sufficient time, and have to have the capability (through reaction or as a catalyst) to nucleate an oxide defect and/or void. The first step obviously requires the metal to cross the oxide layer. Bulk oxide diffusion properties of these materials[11] are insufficient to explain the experimental differences: Following the oxide diffusion coefficient values for Cu and W, a much lower reactivity is expected for W than for Cu. Experimentally, the Cu reactivity is about the same as the reactivity measured for W, or even slightly below it. This seems to rule out bulk diffusion as the predominant mechanism that transports metal through the oxide layer. It has to be noted that the bulk diffusion data available are based on experiments with continuous metal films on top of a thermal oxide.[11] Under such conditions we find decomposition only around the pattern edges, i.e., where the structure exhibits the most significant stress and where it becomes discontinuous. For all other metals investigated here the films become discontinuous upon annealing.

Diffusion through or to preexisting defects in the oxide film can be imagined to enhance metal transport through the oxide. Even good quality thermal oxide films have been found to contain microchannels or holes, as evidenced by TEM.[24–26] Positron annihilation studies[27] suggest that small microvoids (10–20 Å diameter) exist in thermal oxide. These microvoids or channels could be sites which nucleate voids. It is through that kind of intrinsic oxide defect that metal atoms might be able to migrate very efficiently through an oxide as thin as 200 Å. The oxide defects reduce the thickness to be crossed to reach the interface. This effect should be enhanced significantly by stresses in the oxide due to thick patterned films or islands on the oxide. These stresses might even create new microchannels or increase the preexistent ones leading to cracks through the SiO_2 layer. Significant stress levels will build up during the high-

temperature anneal because of the different thermal expansion coefficients of the oxide and the metal on top. Stress enhanced diffusion might contribute to what we have observed for a thick film of tungsten where the decomposition occurs around the metal pattern, where the stress is expected to be maximal (Fig. 5). More support comes from the HRTEM picture of the aggregated W film (Fig. 3), where only a small fraction of the W islands nucleated a void. This may suggest that only if locally enhanced stress and the metal source coincide with an existing oxide defect can oxide voids be nucleated. Thermodynamically, the formation of SiO at the interface may require the presence of small free volumes, because the major decrease in free energy upon SiO formation originates in the entropy term for *gaseous* SiO.[14] SiO gas formation inside a bubble or channel could locally increase the pressure there until the remaining intact oxide layer above cracks. As soon as there is a direct path between the interface and the surface of the oxide, further void growth is known to proceed rapidly.[10] Microdefects are a very probable source for void formation, especially when enhanced through film stress. The combination of the two phenomena might explain the differences found in the densities of voids ($\simeq 10^3$ mm^{-2}), the densities of microchannels or microvoids ($\simeq 10^8$ mm^{-2}), and the densities of metal islands ($\simeq 10^7$ mm^{-2}). No model has been published until now that tries to explain these density differences.

Once the metal has reached the interface it enhances the oxide decomposition. A very nice example for this effect, completely decoupled from the metal diffusion through the oxide, is seen in Figs. 3 and 4. Tungsten particles on top of an oxide layer generally do not damage the oxide enough to cause oxide decomposition beneath them (Fig. 3). But once a void has been nucleated by an interplay of stress and intrinsic defects somewhere on the sample, the growing circumference of the void will reach the tungsten particles still present on the surface. What happens then is most pronounced for tungsten, probably because of the low diffusion coefficient of tungsten through the oxide as well as across the surface. When the void circumference reaches a tungsten particle the void growth rate is locally enhanced dramatically, leading to a rugged looking edge of the void: the cauliflower appearance seen in Fig. 4. Especially in the case of tungsten this leads to strongly enhanced void diameter growth rates. The enhancement of the void diameter growth rate is found for all the metals analyzed here. Some of them show a much enhanced void density as well, such as, e.g., Cu, which must be a result of the faster diffusion through the oxide. The question that remains to be answered is which property of the metal is responsible for the decomposition enhancement?

It was shown that the enhancement of oxide decomposition found for tungsten requires the metal to reach the Si/SiO_2 interface. To address the question, what large quantities of metal at the interface would do to the decomposition process, we used thermally oxidized tungsten silicide films as substrates. The silicide is, of course, chemically different from the elemental tungsten that was deposited *in situ* on top of the oxide. A WSi_2 substrate beneath SiO_2 shows a surprisingly small oxide decomposition rate (Fig. 6); only very thin (≤ 3 Å) elemental tungsten layers deposited on top of the oxide show a comparatively low decomposition enhancement. This weak effect, which is also seen for other silicides, shows that metal atoms are more active when they are not associated with silicon. In the case of the oxide decomposition enhancement by metals on top of the oxide, metal atoms reach the SiO_2/Si interface where they react. The reaction of the metal with the silicon is to form a silicide. The reaction will release energy as well as change the electronic configuration of the metal. The energy released upon reaction may be used to help decompose SiO_2 and Si to SiO and thus speed up void formation. Alternatively, the electronic configuration of the metal may permit charge transfer to, e.g., break Si—O bonds, where the silicide cannot.

Almost all the transition metals studied here react strongly with silicon. Some of them react even when deposited at room temperature, others form silicides when annealed to temperature well below 1000 °C (Ref. 28) (except Ag, which does not seem to react). This reaction will change the electronic configuration of the metal as well as release energy; both might enhance oxide decomposition. The initial sp^3 silicon hybridization is changed upon reaction with transition metals yielding a new electronic configuration involving the *d* electrons of the metal. The metal *d*-band electronic states generally move away from the Fermi level when a silicide is formed.[29] It has also been proven that silicon diffuses very easily through most of their silicides or the metals to form a thin film of silicon on the surface.[30] Upon contact with silicon we therefore expect the metal electronic states to undergo dramatic changes, all in the direction of reducing the density of states close to the Fermi level. The heat of formation of silicides will also have a general trend towards higher values from Ag to Pt. From silver to platinum the maximum of the density of *d* electrons has a tendency to move toward the Fermi level. The increase of electron density, nearby the Fermi level reflected by the electronic heat capacity (Table I), can explain the trend of the reactivity of these metals in the oxide decomposition enhancement; more electrons are available to induce the bonding change of silicon atoms and more energy will be released upon bond formation. The two effects (changes in band structure and heat of formation) are, of course, intimately related and are probably at the origin of the oxide decomposition reaction. The main question that remains to be answered is whether the metal can serve as a catalyst or is consumed during the reaction.

To explain oxidation rate changes of silicides or silicon in metal-rich environment, a mechanism involving the electronic structure has been described.[31] For the case of Au and Pt, a catalytic effect on the oxidation has been demonstrated based on the particular electronic configuration of the silicon atoms.[32] In our case we might be confronted with the reverse reaction which can be enhanced by electronic processes similar to the one that explain the catalytic oxidation of silicides.[33] For the oxide decomposition reaction it is at present not clear if

the metal at the interface acts as a catalyst or not, but it appears as if the decomposition occurs much slower once a silicide has been formed. This leads us to assume that the metal here is consumed in the process of decomposing the oxide.

In conclusion, we have clearly demonstrated that metal impurities can drastically change oxide integrity upon vacuum anneal. They induce an enhanced oxide decomposition following two different mechanisms, depending on the electronic properties of the metal. The first class of materials reacts directly with the SiO_2 and causes homogeneous decomposition, thinning down the oxide from the surface. For the second class the metal needs to get to the interface and an inhomogeneous decomposition via voids is the consequence, based on defects in the oxide that may help the metal diffuse to the interface. Microchannels or microvoids in the oxide might be such defects. They seem to need additional enhancement through, e.g., film stress to significantly influence metal diffusion through the oxide. The efficiency of the process at the interface seems to be correlated to the electronic configuration of the metal.

ACKNOWLEDGMENTS

We gratefully acknowledge valuable discussions with F. M. d'Heurle, O. Thomas, and G. W. Rubloff. The help of G. B. Bronner, F. K. LeGoues with TEM, E. A. Irene with the preparation of the oxidized silicide samples, and the IBM Yorktown Silicon Facility is greatly appreciated. This work has been supported in part by the Office of Naval Research, U. S. Department of Defense. One of us (H.D.) acknowledges the financial support of Equipe de Recherche No. 388 associée au Centre National de la Recherche Scientifique.

---

*Permanent address: Groupe de Physique des Etats Condensés, Département de Physique, Facultés des Sciences de Luminy, Université d'Aix-Marseille II, Case Postale 901, 13288 Marseille CEDEX 09, France.

[1]B. R. Singh and P. Balk, J. Electrochem. Soc. **125**, 453 (1978).
[2]R. Tromp, G. W. Rubloff, P. Balk, F. K. LeGoues, and E. J. van Loenen, Phys. Rev. Lett. **55**, 2332 (1985).
[3]G. W. Rubloff, K. Hofmann, M. Liehr, and D. R. Young, Phys. Rev. Lett. **58**, 2379 (1987).
[4]M. Kobayashi, T. Ogawa, and K. Wada, Proceedings of the Electrochemical Society Spring Meeting, Toronto, 1985, p. 94.
[5]M. Liehr, G. B. Bronner, and J. E. Lewis, Appl. Phys. Lett. **52**, 1892 (1988).
[6]M. Liehr, H. Dallaporta, and J. E. Lewis, Appl. Phys. Lett. **53**, 589 (1988).
[7]F. W. Smith and G. Ghidini, J. Electrochem. Soc. **129**, 1300 (1982).
[8]R. E. Walkup and S. I. Raider, Appl. Phys. Lett. **53**, 888 (1988).
[9]S. T. Ahn, H. W. Kennel, W. A. Tiller, and J. D. Plummer, J. Appl. Phys. **65**, 2957 (1989).
[10]M. Liehr, J. E. Lewis, and G. W. Rubloff, J. Vac. Sci. Technol. A **5**, 1559 (1987).
[11]J. D. McBrayer, Ph.D. thesis, Stanford Electronics Laboratories, Stanford University, Stanford, California, 1983.
[12]Japanese Patent No. LOP-52-69571, Hitachi Corporation (9 June 1977).
[13]U. S. Patent 4,053,335, IBM Corporation (11 October 1977).
[14]F. M. d'Heurle (private communication).
[15]C. Y. Ting, M. Wittmer, S. S. Iyer, and S. B. Brodsky, J. Electrochem. Soc. **131**, 2934 (1984).
[16]R. S. Bauer, R. Z. Bachrach, and L. J. Brillson, Appl. Phys. Lett. **37**, 1006 (1980).
[17]E. A. Alessandrini, D. R. Campbell, and K. N. Tu, J. Appl. Phys. **45**, 4888 (1974).
[18]D. D. Wagman, W. H. Evans, V. B. Parker, R. H. Schumm, I. Halow, S. M. Bailey, K. L. Churney, and R. L. Nuttal, *The NBS Tables of Chemical Thermodynamic Properties,* Natl. Bur. Stand. (U.S.) Phys. Chem. Ref. Data, Suppl. 2 (U.S. GPO, Washington, D.C., 1982).
[19]R. Pretorius, J. M. Harris, and M.-A. Nicolet, Solid-State Electron. **21**, 667 (1978).
[20]S. M. Goodnick, M. Fathipour, D. L. Ellsworth, and C. M. Wilmsen, J. Vac. Sci. Technol. **18**, 949 (1981).
[21]H. Kräutle, W. K. Chu, M. A. Nicolet, and J. W. Mayer, *Applications of Ion Beams to Metals* (Plenum, New York, 1973), p. 193.
[22]S. Wright and H. Kroemer, Appl. Phys. Lett. **36**, 210 (1980).
[23]J. F. Morar, B. S. Meyerson, U. O. Karlsson, F. J. Himpsel, F. R. McFeely, D. Rieger, A. Taleb-Ibrahimi, and J. A. Yarmoff, Appl. Phys. Lett. **50**, 463 (1987).
[24]E. A. Irene, J. Electrochem. Soc. **125**, 1708 (1978).
[25]J. M. Gibson and D. W. Dong, J. Electrochem. Soc. **127**, 2722 (1989).
[26]M. Liehr, H. Lefakis, F. K. LeGoues, and G. W. Rubloff, Phys. Rev. B **33**, 5517 (1986).
[27]B. Nielsen, K. G. Lynn, D. O. Welch, T. C. Leung, and G. W. Rubloff, Phys. Rev. B **40**, 1434 (1989).
[28]P. S. Ho, G. W. Rubloff, J. E. Lewis, V. L. Moruzzi, and A. R. Williams, Phys. Rev. **22**, 4784 (1980).
[29]L. Braicovich, I. Abbati, J. N. Miller, I. Lindau, S. Schwarz, P. R. Skeath, C. Y. Yu, and W. E. Spicer, J. Vac. Sci. Technol. **17**, 1005 (1980).
[30]G. W. Rubloff, in *Proceedings of the Materials Research Society Symposium on Thin Films—Interfaces and Phenomena, Boston, 1985,* MRS Symp. Proc. No. 54, edited by R. J. Nemanich, P. S. Ho, and S. S. Lau (MRS, Pittsburgh, 1986), p. 3.
[31]F. M. d'Heurle, A. Cros, R. D. Frampton, and J. A. Irene, Philos. Mag. B **55**, 291 (1987).
[32]A. Cros, J. Derrien, and F. Salvan, Surf. Sci. **110**, 471 (1981).
[33]E. A. Irene and R. Ghez, Appl. Surf. Sci. **30**, 1 (1987).

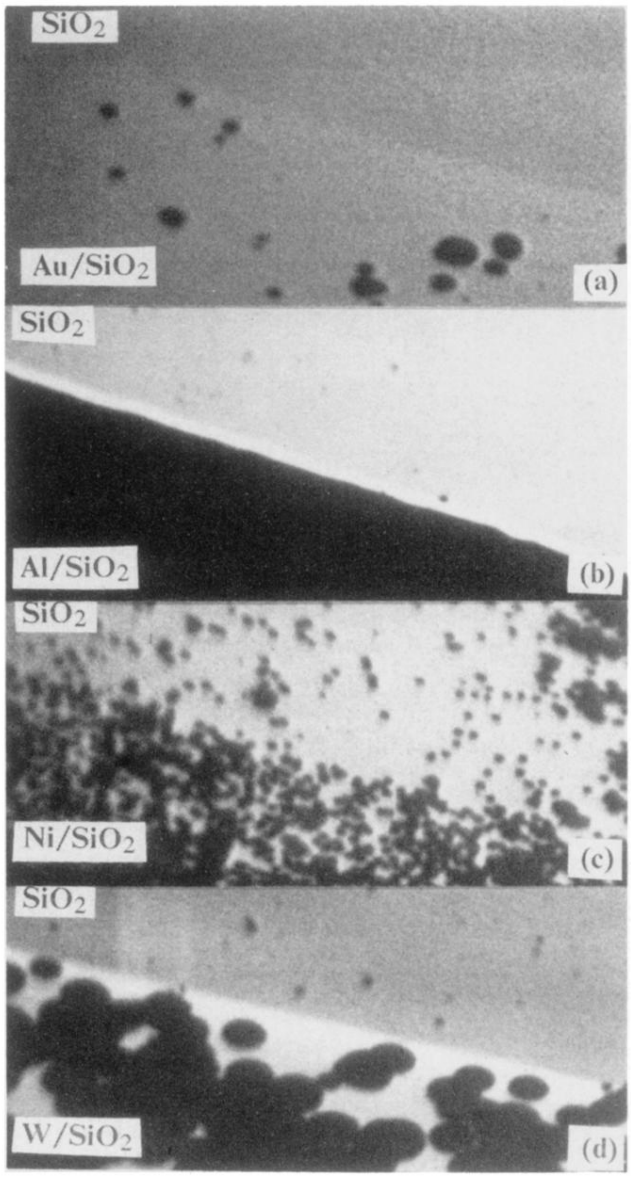

FIG. 1. A sequence of scanning electron microscope pictures taken during ultrahigh-vacuum anneal of a 200 Å SiO_2 layer on Si(100). The field of view is $\simeq 1$ mm by 1 mm, the sample being tilted by $\simeq 60°$ giving circular voids an elliptical appearance. The pictures were taken at 3 keV electron energy and 50 nA beam current in secondary electron mode. The dark areas represent clean Si areas, the bright background the SiO_2 layer. Metals have been evaporated only on the lower half of the samples to allow comparison with clean conditions. (a) shows a layer of 40 Å of Au after anneal to 1000 °C for 15 min; (b) 35 Å of Al after anneal to 1000 °C for 2 min; (c) 3 Å of Ni after anneal to 1000 °C for 50 min; (d) 3 Å of W after anneal to 1000 °C for 30 min.

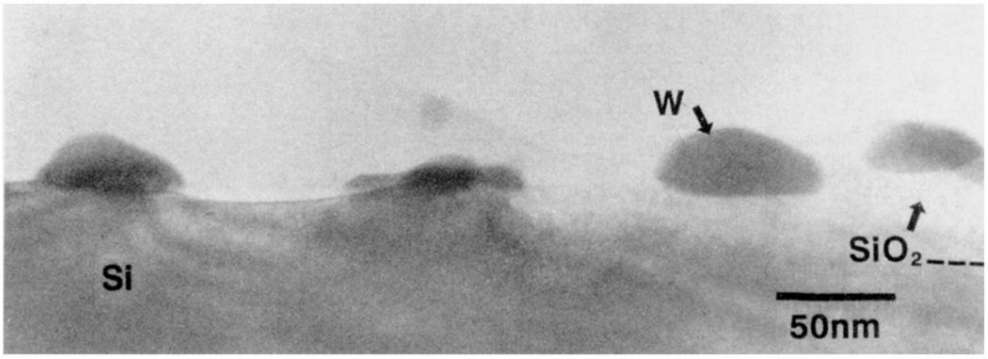

FIG. 3. High-resolution cross-sectional TEM photograph of a 40-Å-thick tungsten layer evaporated on 200 Å of thermal oxide. The sample was vacuum annealed to 1000 °C for 10 min.

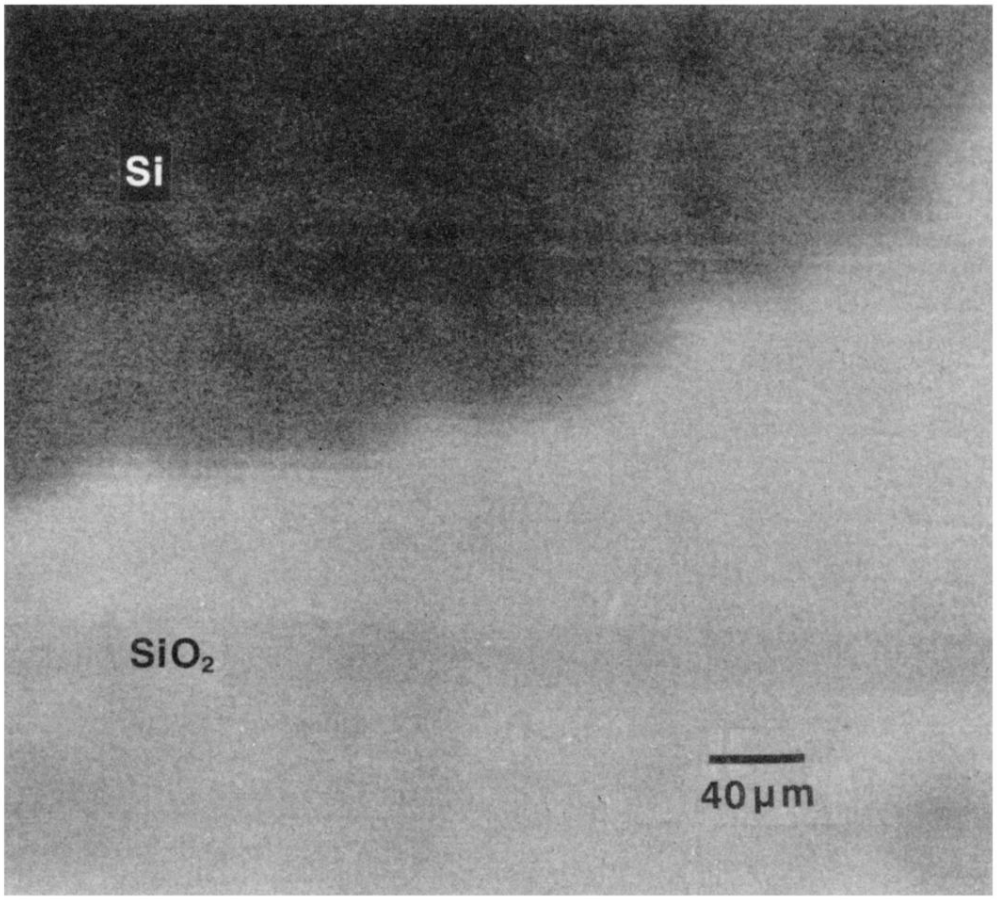

FIG. 4. High-resolution SEM picture of a void edge on a sample with 30 Å tungsten on 200 Å thermal oxide. The sample had been vacuum annealed for 20 min to 1000 °C.

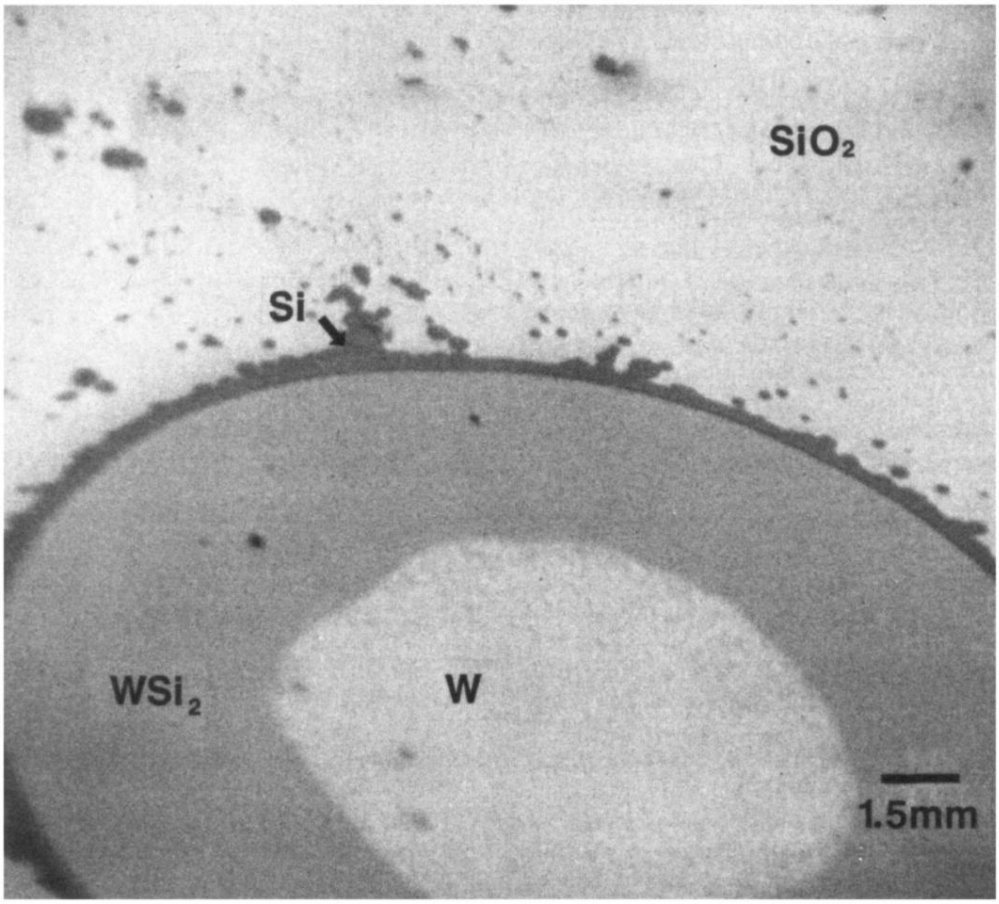

FIG. 5. SEM picture of a 500-Å-thick tungsten dot on 200 Å thermal oxide. The sample has been vacuum annealed to 1000 °C for 12 min. Results of Auger-electron spectroscopic analysis of different areas are indicated.

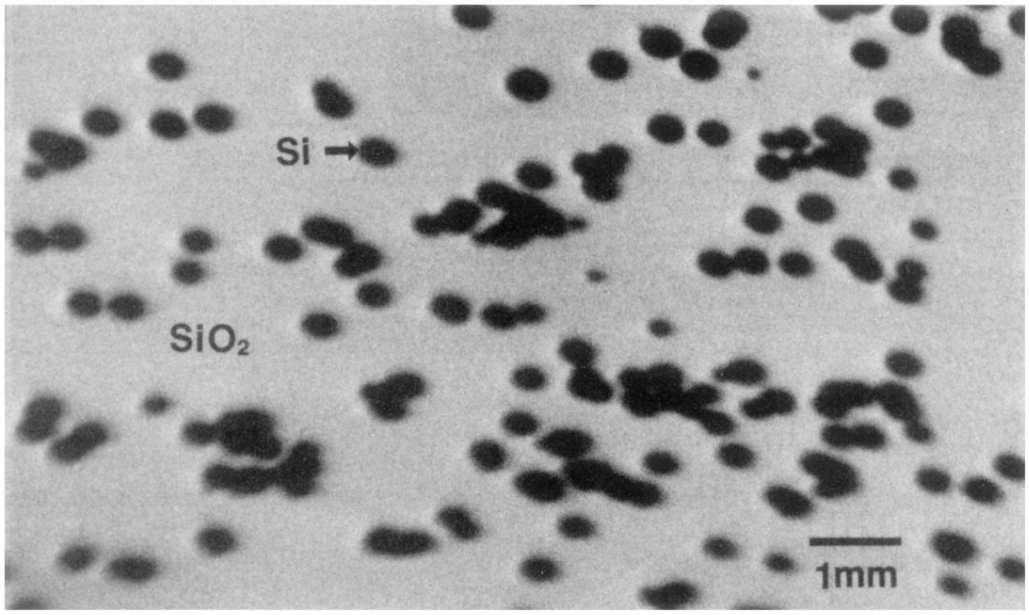

FIG. 6. SEM picture of a Si(100) sample with 1500 Å WSi_2 and 200 Å thermal oxide on top of the silicide. The sample has been vacuum annealed to 1000 °C for 360 min.